

Characterization of Powder Injection Molded Components Using X-Ray CT

David P. Harding, Zhigang Zak Fang, C.L. Lin, Jan D. Miller

**Department of Metallurgical Engineering
University of Utah
135 South 1450 East Room 412
Salt Lake City, Utah 84112**

ABSTRACT

A good understanding of the microstructure of powder injection molded (PIM) components during debinding and sintering is essential in designing and optimizing PIM processes and properties. So far we have been limited in our ability to "see" what is going on. Microstructural characterization has classically been carried out using two-dimensional (2-D) image analysis techniques. This paper introduces a new micro characterization technique using three-dimensional (3-D), X-ray computerized tomography (CT) to characterize PIM parts. The medical profession has long relied on CT scans see inside patients. With the advancement of technology, the same techniques can be applied to metallic materials with multiphase microstructures, for a clearer understanding of microstructure evolution during the processing of these components. This paper discusses these issues and present results from actual PIM component analysis. It also discusses some preliminary method development aimed at quantitative analysis of the microstructure.

INTRODUCTION

Microstructural characterization has conventionally been carried out using 2-D image analysis techniques [1]. These techniques are well defined. Volumetric parameters are typically inferred from linear or area measurements. This approach of deriving 3-D parameters from 2-D measurements has severe limitations because a) error is introduced as with any projection and b) some characteristics are particularly difficult to determine using two dimensional images. For decades the medical industry has used three dimensional tomography imaging devices to "look inside" patients. These devices include CAT scans, MRIs, and ultrasounds. These machines provide 3-D tomographic images based on different physical properties. Other industries are finally following medicine's lead and are using tomographic imaging techniques to research and monitor their processes. New techniques are being developed and commercialized which provide three dimensional micrographs.

At the same time, advances in computer hardware and 3-D computer rendering allows common desktop computers to process and display these three dimensional images. These technological advances have

provided tools for viewing and analyzing internal structure of solid materials directly in three dimensions. The technology has been successfully applied to the study of internal structure of minerals and mineral processing. However, partially due to the limitations with regard to atomic numbers and the dimensional resolution, there is little research to date that applies the 3-D X-ray CT and other 3-D imaging techniques to the microstructural study of metallic materials, including the powder injection molded materials. There is also a lack of analytical tools which use 3-D images and make quantitative measurements of 3-D microstructure features. The microstructure features include volume fraction, linear dimensions, mean free path, contiguity, dihedral angles, and many parameters that are linked to properties of the materials. This research investigates the feasibility of applying the 3-D X-ray micro CT technique to characterize PIM parts, discusses these issues, and present results from analyzing actual metal powder components formed using polymeric binder. Also discussed are some preliminary methods under development aimed at quantitative analysis of the microstructure.

EXPERIMENTAL METHODS

X-ray MicroCT

For this study, a conical X-ray microCT (computed tomography) machine was used. The X-ray microCT is one of many techniques which can produce 3-D tomographic data. However, the quantitative analysis tools used in this study for the X-ray microCT images can be used to analyze obtained by other techniques.

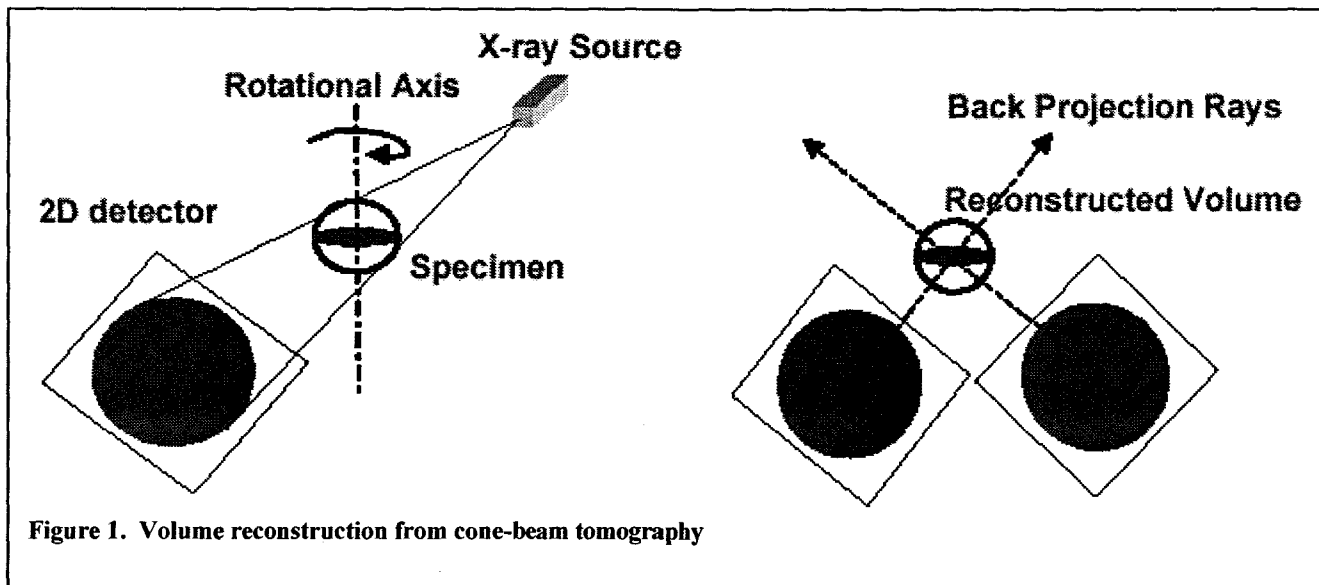


Figure 1. Volume reconstruction from cone-beam tomography

As illustrated in figure 1, the X-ray microCT uses a micro focused X-ray cone beam to make a radiograph of the specimen. The specimen is rotated through 360° and a series of radiographs are recorded. The data is processed using a reconstruction algorithm based on a generalization in three dimensions of the widely used convolution-back projection method. This algorithm produces a three dimensional array of voxels. A voxel is the three dimensional equivalent of a pixel.

The voxel brightness corresponds to a physical property of the material. In X-ray microCT, the brightness, or intensity level, represents the linear attenuation coefficient. The linear attenuation coefficient is based on the electron density and the effective atomic number of the material, which are related to the material density. The X-ray microCT, in effect, produces a 3-D map of the densities inside a sample. The maximum recommended density to be imaged using the microCT at the University of Utah is 8.0 g/cc. [2]

Synthetic Diamond Granules in a Tungsten-Carbide Matrix

Two samples were used for the feasibility study. The first is a composite made from granules of synthetic diamond with a matrix of tungsten-carbide and cobalt. The sample, as imaged, is a green compact with 50 percent by volume polymeric binder. The polymer bound powders are pressed into a thin disc at low heat.

Copper Infiltrated Stainless Steel

A copper infiltrated stainless steel sample was also used in the study. The sample was prepared by 3-D printing -- a solid free form fabrication technique -- of stainless steel powders followed by sintering and infiltrating the compact with copper.

Image Acquisition

A 1.1 mm slice of the steel was sectioned from the center using a hacksaw. The slice and the composite disc were then sectioned into roughly 1.3 mm cubes using shear cutters.

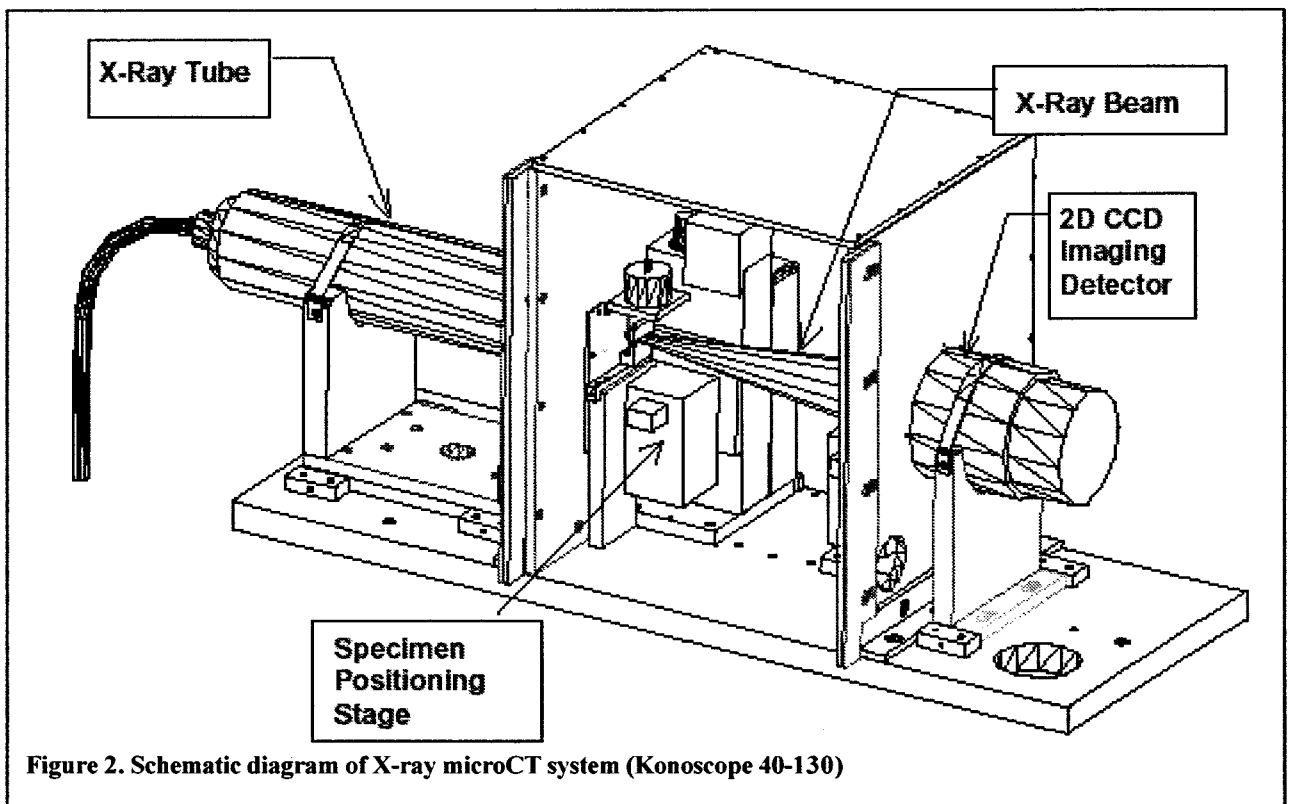


Figure 2. Schematic diagram of X-ray microCT system (Konoscope 40-130)

The samples are placed in the machine for X-ray scan. Figure 2 is a schematic of the microCT used in this study. The specimens were scanned at 130 kV, 0.050 mA, with 8 μm focus spot, with a 32 second exposure time, using a 20 mil brass filter. Once the scans are completed, acquired scan data are transferred from the scan control computer (Mac) to the reconstruction workstation (SGI). There are two programs, system calibration and tomographic reconstruction, to perform calibration and reconstruction processes.

IMAGE ANALYSIS

There are many image analysis routines which are commonly used in two dimensional image analysis which provide useful information about the specimen. All of the information which can be obtained from a 2-D image can also be obtained from a 3-D image, but with higher accuracy. For the full benefit, new methods must be developed for true 3-D measuring, rather than 2-D measurements taken in the three orthogonal directions. The complexities of manipulating three dimensional images are also greater than those associated with 2-D images [3].

Several routines have been investigated so far in this study, and are described below, but many more must be dealt with later [3].

Cropping

Cropping an image is often the first step in image analysis. There may be several reasons to crop an image. Many of the reconstruction algorithms used to generate the three dimensional image data require the volume to have 2^n voxels in each direction, or that both the width and the height must have the same dimension. Because of this, large areas of the three dimensional image may not contain any information. This area can be removed from the image by cropping. Cropping can substantially reduce file sizes and the run time needed by the analysis algorithms. Finally, some specimens are sectioned from a larger sample. Sectioning can damage the new surfaces, which is no longer uniform with the bulk material. Cropping can remove the damaged surface exterior, and allow only the bulk material to be analyzed.

Volume Percent of Components

An important and relatively simple measurement of microstructure is the volume percent of each component. In order to take this measurement it is necessary to identify the different components. The simplest way to do this is using a threshold algorithm. All voxels with intensities within a specific range are identified as a particular component.

A more complex approach to phase classification is based on the rate of intensity change. This approach finds the edges between materials and can help when there are background intensity gradients.

Once the voxels are assigned to a phase then the number of voxels in each phase can be counted and the volume percent can be calculated.

Particle Separation

Individual particles must be identified separately for further measurements. By identifying individual particles, each one can be treated separately in the measurements. For example, without distinguishing between different particles it is impossible to count the number of particles, or calculate their average size.

Particle Size Distribution

A quick measurement of average particle size can be taken by dividing the total volume of the

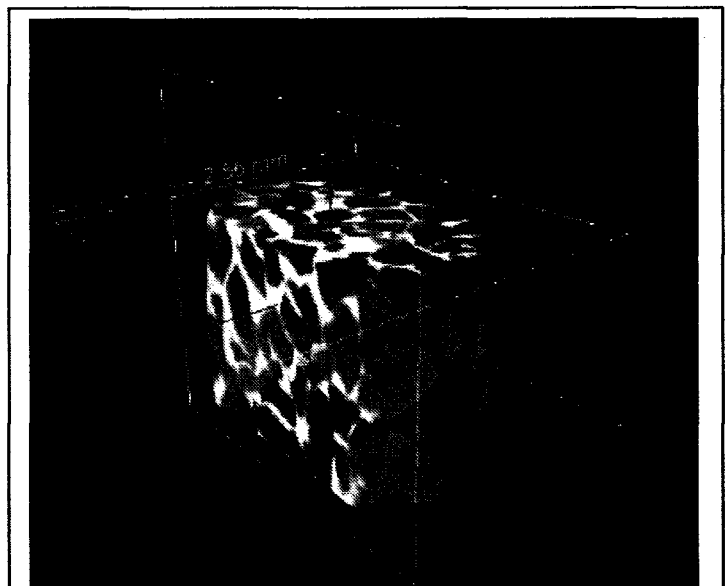


Figure 3. Three dimensional rendering of the X-ray CT image of the diamond/WC-Co composite.

material (number of voxels * volume per voxel) by the number of particles.

Average particle size can also be estimated by counting the number of voxels each particle contains. Since the dimensions of the voxel are known, the size of each particle can be calculated. This approach lends itself well to determining the variance in the particle sizes.

Particle Shape

There are several ways to define a particle shape. One useful shape factor is the ratio between the calculated surface area of the particle if it were a perfect sphere, based on volume, and the measured surface area. If a particle is most spherical then the shape factor will be close to one. The more irregular the shape the lower the shape factor will be.

The surface area of a particle can be measured by counting the number of voxels contained in a particle which border a voxel which doesn't belong to the particle. The accuracy of this measurement is determined by the relative resolution of the image.

RESULTS

Diamond and Tungsten Carbide Composites

The X-ray CT was able to image the diamond/WC-Co. Figure 3 is a screen shot of the rendered diamond/WC-Co specimen. Two clipping planes are added to afford a view of the interior. The dense WC-Co matrix is white and the lighter diamond granules are gray.

Figure 4 shows the results of cropping the image. The image's dimensions are now 100 x 100 x 100 voxels, (about 0.5 mm in each direction). While all of the diamond granules are touching another granule, each one can easily be distinguished by eye.

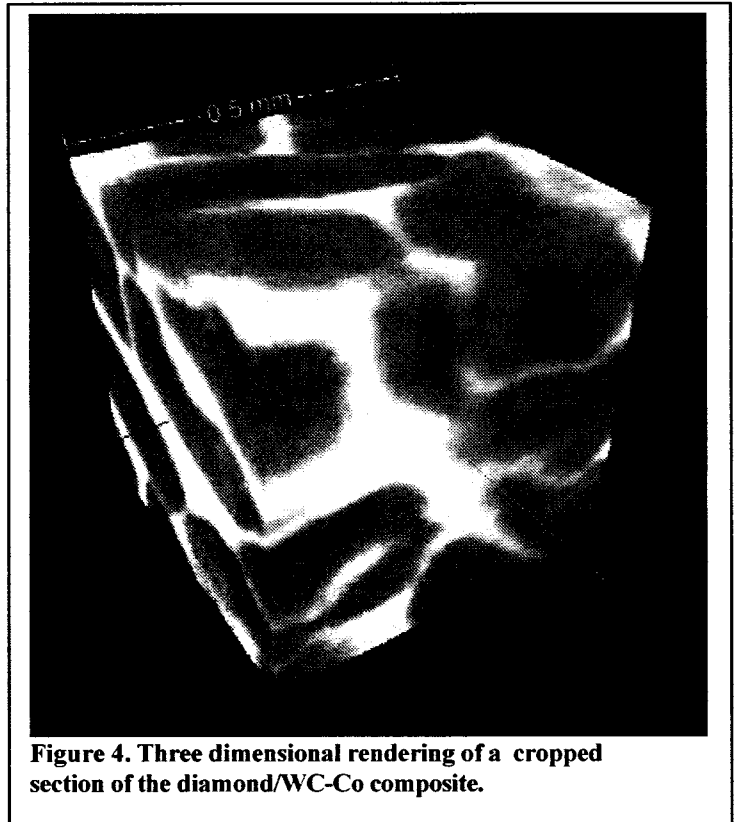
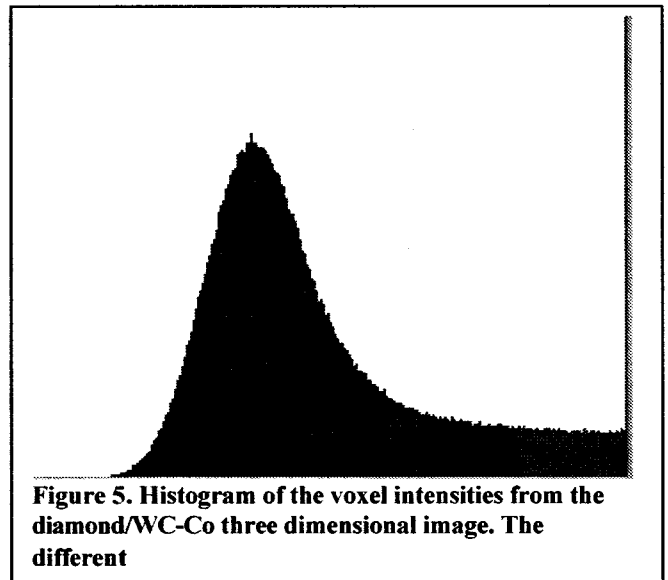


Figure 5 is a histogram of the voxel intensities in the composite image. The WC-Co matrix is over-saturated; most of the WC-Co voxels have the maximum intensity of 255. It is apparent from this graph that there is a distinct difference between the two phases. This makes the phase identification easy.

In this application, the WC-Co matrix is well over the recommended maximum density (14.2 vs. 8.0). Even mixed with polymeric binder at 50 volume percent, the material density is around 11 g/cc. But when mixed with the polymer bound diamond (80 vol%), the overall density drops down to around 4.7 g/cc. The high density of the matrix may cause some artificial



patterns and background intensity gradients, but since the material intensity peaks are so separated the materials can still easily be distinguished.

Figure 6 is a rendered image of the specimen after it has been processed by the threshold algorithm. The matrix has been rendered transparent to allow a view of the diamond granules in the interior.

The image is next processed by separating all of the different diamond granules. This is done by shrinking the granules until they separate from one another. A modified, connected component, recursive algorithm is used to select all voxels which are contiguous and then assigns them a specific gray level. Once all of the granules have been identified, the granules are expanded to their original size. Figure 7 is a rendered image of the separated granules. A random color has been assigned to each gray level to enhance the viewing contrast.

Particle size of the diamond granules are around 200 to 300 μm . But, the average particle size and shape calculations could not be made on this specimen. Only granules which are wholly contained in the image can be included in the calculation. All granules in this cropped specimen were touching the image boundary and were therefore could not be used.

In this aspect the larger relative feature size works as a disadvantage. Less large particles will fit in the same image size when compared with small particles. One obvious solution is to work with a larger image. This would increase the file size, processing time, and in this case is not feasible since there are some unresolved software interfacing problems which limit the size of the images which can be processed to around 100 x 100 x 100 voxels. These interfacing problems should be resolved shortly and larger files (512 x 512 x 512) will be processed.

Copper Infiltrated Stainless Steel

The copper/stainless steel system is a popular powder metallurgy material used for forming dies and molds. Study of this sample revealed limitations of the X-ray microCT technique for characterizing materials of this type. Each 3-D imaging technique, and indeed all imaging equipment, has a range of samples which it can

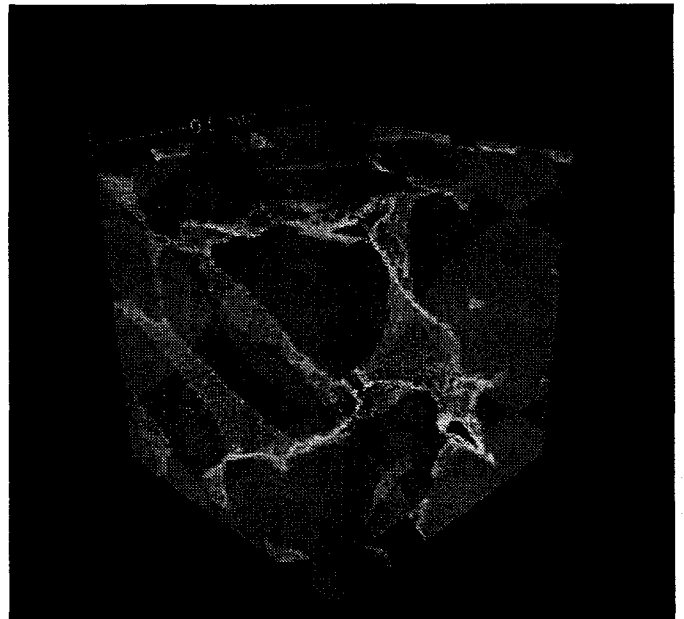


Figure 6. A rendering of the diamond/WC-Co composite. The

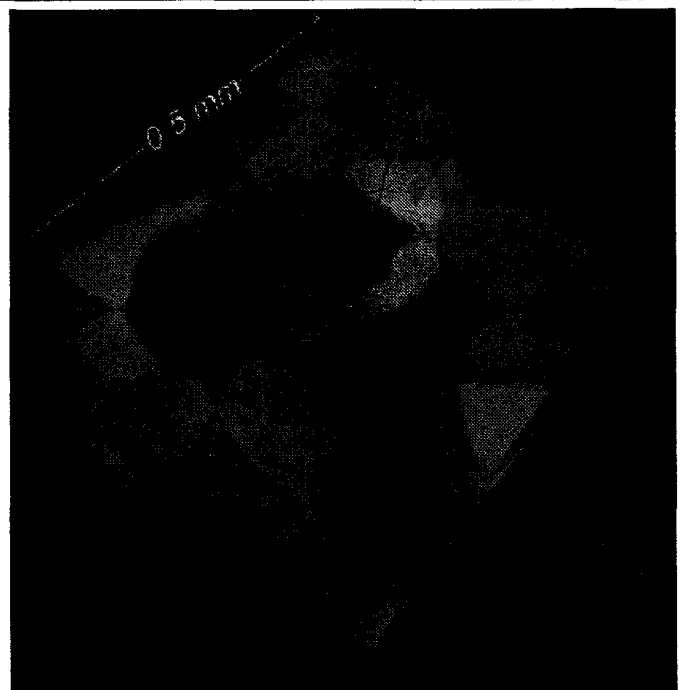


Figure 7. Three dimensional rendering of diamond granules each assigned a random color.

properly image. There are two major reasons why the copper infiltrated stainless steel is not in the range for the X-ray microCT machine used in this study.

Figure 8 shows a rendering of the copper infiltrated stainless steel. The denser copper matrix shows up as a brighter material in between the gray stainless steel particles. The voids show up as darker patches. Two clipping planes have been added to offer a view of the internal structure.

Figure 9 is a zoomed in rendering of a cropped section of the copper infiltrated specimen. The image is 100 x 100 x 100 voxels, which is roughly a half millimeter in each direction. The three phases; void, stainless steel, and copper, can be identified by visual inspection. It is also apparent that the individual stainless steel particles are difficult to distinguish and that the boundary between stainless steel and copper is not well defined. This makes the threshold procedure for identifying materials difficult. The histogram for this image is displayed in figure 10. Ideally there would be three distinct peaks in the histogram, corresponding to the three different phases. In this histogram the voids are mostly separate but blend slightly into the stainless steel intensities. The copper and the stainless steel overlap almost completely. This means that some stainless steel voxels have higher intensity than copper voxels.

The overlap is due to several factors. First, with a voxel size of 5 x 5 x 5 micron, the resolution of the image is close to the size of the stainless steel particles. The particle sizes of the stainless steel powder are approximately 70 μm . This makes edge voxels a particular problem. Since one voxel may contain both copper and stainless steel the intensity comes from a combination of the two materials. When the voids are adjacent to the copper, the edge voxels may have the same intensity as the steel voxels and will be identified as such. These difficulties are inherent in any electronic image analysis process and there are

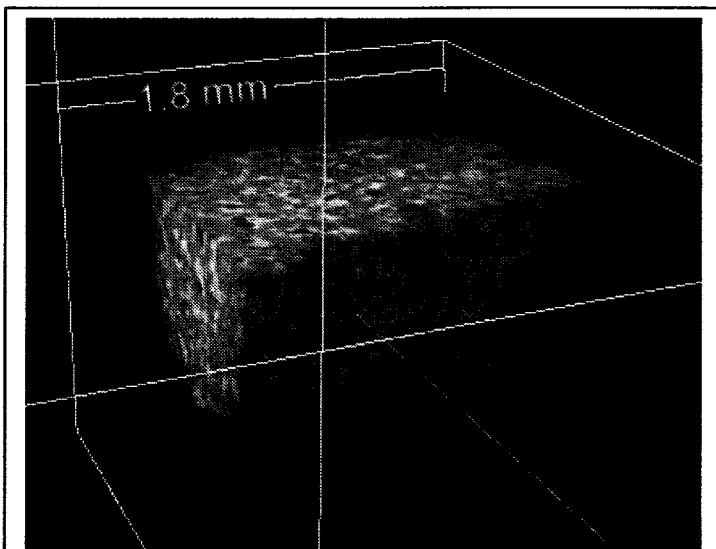


Figure 8. Three dimensional rendering of the X-ray microCT image of copper infiltrated stainless steel.

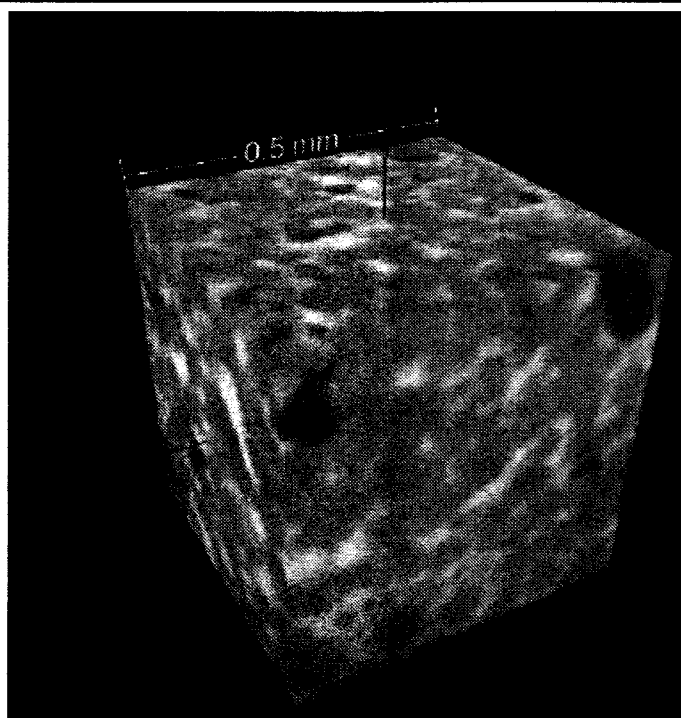


Figure 9. Three dimensional rendering of a cropped section of copper infiltrated stainless steel.

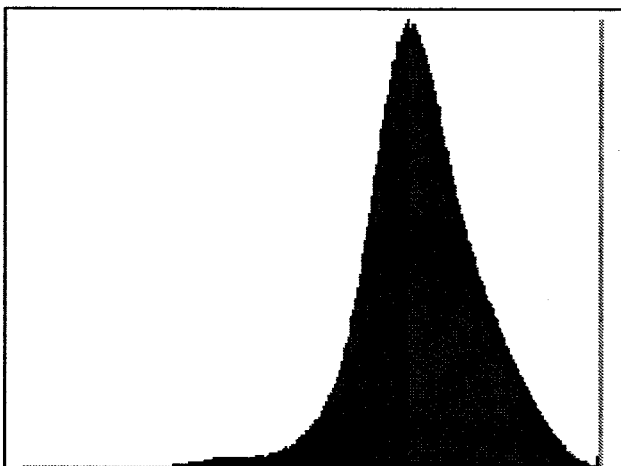


Figure 10. Histogram of the voxel intensities from the copper infiltrated stainless steel three dimensional image. The different colors represent possible component threshold levels.

methods to filter out these problems, but with the resolution so close to the feature size, these filters would wipe out much of the information. At the low relative resolution too many voxels become "edge" voxels.

A second factor is that the densities of copper and stainless steel are somewhat similar, and more importantly, both are near or above the recommended maximum density of 8.0 g/cc. At this high density the X-rays cannot pass through the specimen in adequate quantities. The result is a blurred view of the center of the specimen. The materials in the center of the specimen are recorded with higher intensities than the material on the outsides. This background intensity gradient exacerbates the overlap problem. This gradient can be filtered out, but the routine has not been implemented yet in this investigation.

Figure 11 is a thin slice revealing the interior of the specimen. Due to the background gradient, more of the interior voxels have been incorrectly identified as copper.

DISCUSSION

As it can be seen from above, the X-ray microCT is a powerful tool for viewing the internal structure of multiphase solid materials, particularly composites. However, the resolution and density limits inherent in X-ray imaging are the key difficulties in the application of X-ray microCT to the PIM industry. These limitations are evident from the results presented above.

For powder injection molded parts and indeed most metallic materials, the particle or grain size are on the order of tens of microns down to the sub micron range. To apply the X-ray microCT effectively, the special resolution has to be improved. Spatial resolution on the order of 1 μm can be achieved with the use of synchrotron radiation [4,5,6] rather than the 15 μm resolution produced by conventional microfocus X-ray generators [7]. But synchrotron radiation is expensive and available in only a few locations.

The upper density capability of the X-ray microCT also limits the application to a few light materials. However, green compact of PIM components containing a large volume percent of polymeric binder, or porous materials with large volume fraction of porosity can be evaluated using this technique.

There are alternative methods of producing 3-D tomographical images [8]. Further study could determine if any of these may be of more use in the PIM industry.

SUMMARY

An exploratory study is carried out to study the feasibility of applying X-ray microCT technology to characterize 3-D microstructure of powder injection molded and other powder metallurgy materials. A synthetic diamond and WC-Co composite sample bound by polymer binders and a copper infiltrated stainless material were studied as examples. It is shown that the X-ray microCT imaging technique is a powerful tool for obtaining 3-D data. It can show the 3-D structure of PIM composites. Microstructure parameters such as volume fraction are measured directly from 3-D images. However, the applicability of

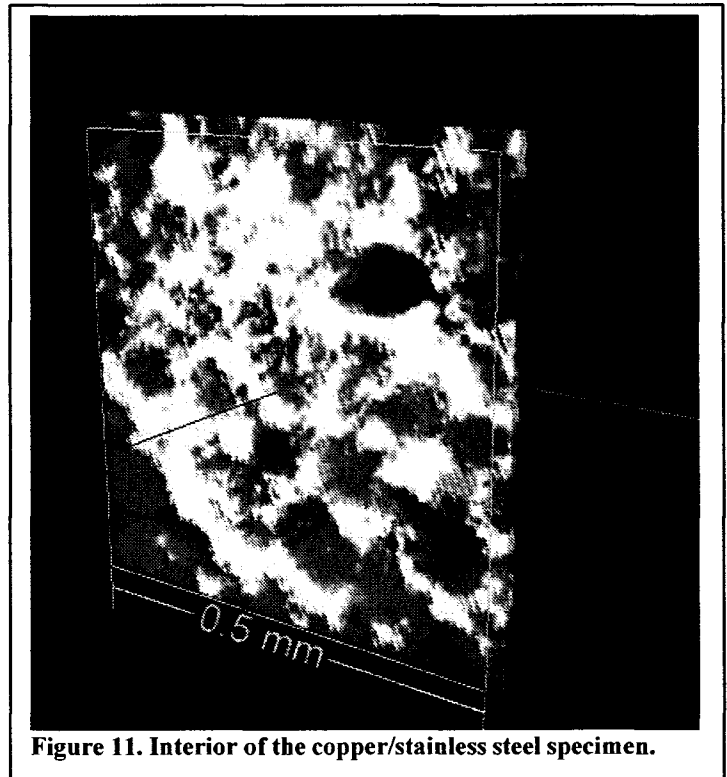


Figure 11. Interior of the copper/stainless steel specimen.

the X-ray micro CT technique is limited by its dimensional resolution, which is approximately 15 microns, and the upper limit on the density of the material (8.0 g/cc) above which the current system is incapable of sufficient penetrating. Current efforts are directed toward developing quantitative analysis tools that can derive microstructure parameters from the 3-D images. There are other techniques for obtaining the 3-D data which could be used for quantitative analysis.

REFERENCES

1. Underwood, E. E. *Quantitative Stereology*, Addison-Wesley, Reading, MA, 1970
2. Lin, C.L., Miller, J.D. "A New Cone Beam X-ray Microtomography Facility for 3D Analysis of Multiphase Materials" 2nd World Congress on Industrial Process Tomography, 2001
3. Nikolaidis, N. and Pitas, I. *3-D Image Processing Algorithm*, John Wiley & Sons, New York, NY, 2001
4. Grodzins, L. "Optimum Energies for X-ray Transmission Tomography of Small Samples – Applications of Synchrotron Radiation to Computerized Tomography I", *Nucl. Instrum. Meth.*, Vol. 206, 1983 pp.541-545.
5. Flannery, D.P., Deckman, H.W., Roberg W.G., D'Amico, K.L. "Three-dimensional X-ray Microtomography", *Science*, 1987, Vol. 237, pp.1439-1444.
6. Kinney, J.H., Johnson, Q.C., Saroyan, R.A. "Energy-Modulated X-ray Microtomography", *Rev. Sci. Instrum.*, 1988, 59 (1), pp. 196-197.
7. Feldkamp, L.A., Jasion, G. "Three-dimensional X-ray Computed Tomography, *Review of Progress in Quantitative Nondestructive Evaluation*", ed. by D.O. Thompson and D.E. Chimenti, Plenum Press, New York, Vol. 8A, 1986, pp. 555-566.
8. Alkemper, J. Voorhees, P. W. "Quantitative Serial Sectioning Analysis", *Journal of Microscopy*, Vol. 201 2001, pp. 388-394.